Journal of The Electrochemical Society, **164** (12) A2812-A2822 (2017)
0013-4651/2017/164(12)/A2812/11/$37.00 © The Electrochemical Society

A Comprehensive Study of Manganese Deposition and Side Reactions in Li-Ion Battery Electrodes

Yoon Koo Lee,[a] Jonghyun Park,[*,b] and Wei Lu[*,z]

Department of Mechanical Engineering, University of Michigan, Ann Arbor, Michigan 48109, USA

A thorough investigation of both manganese (Mn) deposition onto graphite and its side reactions was conducted based on complementary techniques including CV, EIS, GCPL, ICP-OES, SEM and EDS. Each measurement revealed a specific aspect of the degradation phenomena, which taken together all pointed in a common direction. This study focused on 1) deposition mechanisms and effects of manganese ions on the SEI layer; 2) the effects of manganese deposition on electrochemical performance; and 3) direct observation of decomposed layers induced by manganese deposition. It was confirmed that adding $Mn(PF_6)_2$ salt in the electrolyte results in severe capacity decrease and impedance rise. It is found that manganese ions in the electrolyte participate to generate Mn-containing SEI layers when depositing onto the graphite surface accompanied by additional side reactions. Interestingly, before manganese ions deposit onto the graphite electrode, they enhance cell capacity due to additional oxidation reactions. It is found that the reaction of manganese ions changes with the voltage conditions during charge or discharge and the lithiation status of the graphite electrode.
© 2017 The Electrochemical Society. [DOI: 10.1149/2.1851712jes] All rights reserved.

Manuscript submitted June 6, 2017; revised manuscript received September 5, 2017. Published September 16, 2017.

Spinel $LiMn_2O_4$ (LMO) is one of the most widely used commercialized cathode materials because of its low cost, environmental friendliness, high electronic/ionic conductivity, and excellent rate capability and safety.[1] However, this material exhibits significant capacity fade during cycling or storage at elevated temperatures. Several mechanisms of capacity fade have been proposed,[2] and manganese dissolution is one of the most important causes, especially at elevated temperatures.[3,4] Manganese dissolution can be attributed to several possible mechanisms: 1) the disproportionation reaction of manganese ($2Mn^{3+} \rightarrow Mn^{4+} + Mn^{2+}$) becomes faster at high temperatures, and Mn^{2+} ions are soluble in the electrolyte;[5] 2) manganese dissolution accelerates at high voltage due to acids from the oxidation of the solvent molecules;[6] and 3) the solubility of manganese ions increases due to phase transition at high or low voltage regions during cycling.[7] Manganese dissolution leads to loss of active material, structural instability, and rise of ohmic resistance. All these are directly related to capacity fade of the LMO cathode material.

Moreover, dissolved manganese ions are deposited onto the graphite anode and can deplete the lithium in the anode out.[8] Consequently, the overall capacity is decreased. Several studies, however, showed that lithium deintercalation due to manganese deposition could not completely explain the capacity decrease. There must be accompanying side reactions related to manganese deposition—this is critically responsible for the capacity decrease of the graphite electrode.[9–11] For instance, electrochemical impedance spectroscopy (EIS)[12] and cyclic voltammetry (CV)[11,12] were applied to observe side reactions originating from manganese deposition. The accumulation of manganese on the electrode surface was confirmed by different measurement techniques such as X-ray photoelectron spectroscopy (XPS),[10,13] X-ray absorption spectroscopy (XAS),[14,15], secondary ion mass spectrometry (SIMS),[16,17] inductively coupled plasma – optical emission spectroscopy (ICP-OES),[10] electron probe microanalysis (EPM),[10] scanning electron microscopy (SEM)[18] and energy dispersive spectroscopy (EDS).[18] These results were measured either by dissolving manganese ions from the cathode material or by adding salt-containing Mn^{2+} ions in the electrolyte. However, Shilina et al. recently argued that Mn^{3+} not Mn^{2+} is the dominant species dissolved from the $LiMn_2O_4$ material while Mn^{2+} is predominant for the $LiNi_{0.5}Mn_{1.5}O_4$ material.[19] This result is contradicting to the previous knowledge that Mn^{2+} ions are the only soluble species that dissolve from the $LiMn_2O_4$ cathode material. While this aspect needs to be investigated further, it was quite clear that additional manganese was observed with decomposed electrolyte products in the SEI layers of the graphite surface under various experimental conditions.

There are several studies focused on manganese contamination of graphite materials. The catalytic effect of deposited products toward solvent reduction was proposed as an additional capacity fade phenomenon.[11,20] Several XPS measurements were conducted to enlighten the mechanisms of manganese deposition by elucidating the chemical state of the manganese in the SEI layer of the graphite. The oxidation state of manganese present in the SEI layer of the graphite differs from the literature in the case of Mn metal,[12,21–23] Mn^{2+} or Mn^{3+}.[4,14,20] Previous studies still suspected that the metallic state of manganese induces solvent reduction on the graphite surface.[11,20] The reasons for this speculation owe to the fact that 1) Mn metal was found from XPS measurement;[12,21] 2) Mn^{2+} and Mn^{3+} (a form of $MnCO_3$, MnO_2 or Mn_2O_3) does not possess sufficient electronic conductivity to induce additional electrolyte decomposition;[4,20] and 3) capacity fade solely due to manganese reduction is too small and cannot explain continuous capacity decrease.[9,10] Accordingly, manganese ions reduce to manganese metal and then re-oxidize with electrolyte to form manganese compounds which cause significant capacity fade due to higher conductivity of the metallic surface. On the other hand, a recent study proposed that a metathesis reaction took place between Mn^{2+} and some species from the SEI layer, rather than reduction reactions which led to the formation of metallic manganese.[13,14] It is suggested that the manganese oxidation state does not depend on chemical potential or reactions during the discharge/charge process. The researchers proposed an ion-exchange model for manganese deposition on the graphite anode. From the XPS measurement, the manganese compound formed on the anode surface was identified as MnF_2 and $MnCO_3$, which was not affected much by the reductive/oxidative conditions.[13] Currently, the oxidation state of manganese in the SEI layer and the mechanisms of manganese deposition are still being debated in the literature.

Recently, researchers tried to investigate why different oxidation states of manganese in the graphite were observed. One of the previous studies conducted experiments to determine the effect of manganese contamination on the SEI layer.[20] They claimed a two-step process involving manganese deposition in which Mn^{2+} reduces to Mn^0 in the first step, followed by the re-oxidation of Mn^0 converting to $MnCO_3$. This is a possible reason why different oxidation states of manganese can be observed. Another study proposed that the oxidation state of manganese depends on the lithiation state of graphite.[24] They claimed that manganese is present as Mn^{2+} ions in the delithiate graphite electrode whereas it is in a reduced state in the lithiated graphite electrode. They also proposed that Mn^{2+} ions are transported as neutral

*Electrochemical Society Member.
[a]Present Address: Battery R&D, LG Chem Gwacheon R&D Center, Gyeonggi-do 13818, Korea.
[b]Present Address: Department of Mechanical and Aerospace Engineering, Missouri University of Science and Technology, Rolla, Missouri 65409, USA.
[z]E-mail: weilu@umich.edu

Downloaded on 2017-12-01 to IP 35.3.99.1 address. Redistribution subject to ECS terms of use (see ecsdl.org/site/terms_use) unless CC License in place (see abstract).

complexes in which the cation is chelated by carboxylated groups. This complex is sufficiently bound to avoid cation exchange in the outer SEI layer so that it reaches the inner layer where Mn^{2+} ions can be chemisorbed at the surface with the oxidation state of Mn^0 or Mn^1. Vissers et al. also proposed a similar hypothesis that manganese ions deposit onto the outer surface of the inner inorganic SEI layer in which the manganese ions are reduced from an oxidation state of 2 to an oxidation state of 1 during lithiation of the graphite.[17] Wandt et al. proposed that the oxidation state of manganese can be changed with different environmental conditions.[15] During operating conditions, the oxidation state of manganese is found to be 2+ both on lithiated and de-lithiated graphite, whereas manganese is found to be in metallic state with ex-situ analysis. From these observations it can be inferred that the oxidation state of manganese in graphite is sensitive to the conditions of samples and the lithiation state of the graphite electrode.

The objective of this study is to investigate the effect of manganese deposition and its side reactions on the graphite anode. In order to achieve a comprehensive understanding of the complicated mechanisms of manganese deposition on graphite electrode, multiple complementary measurements were applied under various experimental conditions. From the previous literature, we found that the oxidation state of manganese in graphite is sensitive to the conditions of samples and the lithiation state of the graphite electrode.[15,20,24] Therefore, fresh, lithiated and de-lithiated graphite samples were prepared to differentiate the possible mechanisms of manganese deposition on graphite samples of different conditions. Cyclic voltammetry and EIS were performed to differentiate the oxidation/reduction reactions and to identify the corresponding manganese contamination mechanisms on SEI layers. The amount of deposited manganese, capacity and impedance were quantitatively measured to elucidate the impact of manganese deposition on the graphite electrode. Finally, mechanisms of the formation of manganese compounds were proposed based on the experiments.

Experimental

Since individual measurement techniques provide only limited information about a certain phenomenon, we employed multiple complementary measurements in various experimental conditions to achieve a comprehensive understanding of manganese deposition. Several electrochemical measurement techniques, such as CV, EIS and capacity measurement, were employed to investigate how manganese ions influence the graphite electrode in terms of cell performance and capacity retention. Additional measurements such as ICP-OES, SEM and EDS were performed to strengthen the hypothesis made from the electrochemical measurements. In this work we focused on three main topics in order to investigate both manganese deposition and consecutive side reactions. These include 1) reaction mechanisms and effects of manganese ions deposition on the SEI layer; 2) effects of manganese deposition on the electrochemical performance; and 3) direct observation of decomposed layers induced by manganese deposition.

First, interactions between manganese ions and the SEI layers were investigated. In this work, fresh and formation-cycled graphite electrodes were both prepared to differentiate the impact of manganese ions on the graphite with and without SEI layers. Generally, the manganese ions are generated from the dissolution of the cathode materials; thus, transport and deposition into the anode are expected after the formation of the SEI layer. However, an investigation of the impact of manganese ions while forming the SEI layer would provide a contrast to the reaction of manganese deposition after SEI layers are already formed. Also, the SEI layer itself is not a robust structure, especially at high temperatures. Consequently, the amount of manganese ions from the accelerated dissolution may have an impact on the reformation of SEI layer due to its instability. By comparing the interactions between fresh and formation-cycled graphite electrode with manganese ions in the electrolyte, mechanisms and impact of manganese ions on the SEI layer will be better understood. To do so, cyclic voltammetry, galvanostatic cycling with potential limitation (GCPL) and EIS were applied. By applying different measurement techniques to the graphite samples, different aspects of electrochemical reaction can be identified. Second, electrochemical measurements and ICP-OES measurements were performed to quantify the effect of manganese deposition. After cell capacities and impedances were identified, ICP-OES measurements were carried out to measure the exact amount of manganese deposited on the graphite. By comparing the amount of deposited manganese and changes in capacity and impedance, the connections between manganese deposition and their influence on cell performance were investigated. In addition, separate experiments were performed to measure the amount of lithium extracted from the graphite anode due to manganese ions. These experiments can provide information parallel to previous experiments with regard to the Mn-Li exchange mechanism.

Finally, in order to examine whether manganese actually induces side reactions and forms decomposed layers, manganese metal surface was observed. Previous studies have shown that manganese deposited onto the graphite surface was detected by various techniques such as XPS,[12] SIMS,[16] ICP-OES and EPM.[10] In turn, it was proposed that the decomposed layer would be formed due to drastic decomposition of the electrolyte on the manganese metal surface.[12] In this work, in order to clearly observe the decomposed layers formed on the metallic state of the manganese surface, the graphite electrode was replaced with a manganese metal. Both fresh and cycled manganese metal surfaces were directly observed to see whether manganese is responsible for forming decomposed layers using the scanning electron microscope (SEM). Elemental analysis was also conducted on these samples using energy dispersive spectroscopy (EDS) to confirm that metallic states of manganese form an additional passivation layer with electrolyte decomposition products.

Sample preparation.—Fresh graphite negative electrodes were made from graphite powder (TIMREX SLP30, TIMCAL) and PVDF (Kureha KF 7208) binder in a weight ratio of 90:10. They were mixed together in a Speedo Mixer (FlackTek Inc.) for 15 minutes. The mixed slurry was coated on a thin copper foil and dried in vacuum at 100°C for 24 hours, then transferred into an argon-filled glove box (MBraun) with less than 0.1 ppm of oxygen and moisture in order to avoid exposure to ambient air. Next, graphite electrodes were assembled to sealed 2032 type coin cells (MTI) with a lithium foil (Alfa Aesar) counter and reference electrode with a separator (Celgard 2320). We did not confirm the water content in the electrolyte, but followed careful preparation procedures to avoid exposure to moisture. In order to reduce any possible impact of manganese ions on the lithium metal, an excessive amount of lithium foil was used. Moreover, dissolved manganese ions were mostly on the graphite anode. Vissers et al.[17] investigated the manganese exchange reaction and found with ICP-MS that the SEI layer will sequester the manganese ions from the electrolyte. Their results revealed that each of the primary constituents of the inner iorganic SEI layer was able to sequester manganese ions from the electrolyte. In the case of Li_2CO_3-containing electrolyte which is a known constituent of the SEI layer, the concentration of manganese was dropped by a factor of 1488 from 38.700 to 0.026 ug/g. Due to the these reasons, we assume that the interaction between manganese ions and the lithium metal is negligible.

Formation cycling was performed by the first three cycles from 1.5 V to 0.01 V at a rate of C/10 using a battery testing system (VMP3 multi-channel potentiostat, Biologic). Next, lithiated and delithiated graphite was achieved by holding the voltage at 0.1 V and 1.0 V for 3 hours, respectively. Finally, the cycled cell was disassembled in the glove box and reassembled with the electrolyte possessing different concentrations of manganese for further experiments.

According to the previous literature, the amount of manganese dissolved from the cathode electrode has been measured under different storage and cycling conditions. The amount of manganese dissolved is affected by the applied potential, charge/discharge conditions, operating temperature, carbon content, calcination temperature and surface area of the cathode particle, and so on.[6,25–27] Depending on the operating conditions, the amount of dissolved manganese can vary from 30 ppm[6] to 1500 ppm[26] after 50 cycles at room temperature

Downloaded on 2017-12-01 to IP 35.3.99.1 address. Redistribution subject to ECS terms of use (see ecsdl.org/site/terms_use) unless CC License in place (see abstract).

conditions. Jang et al. measured about 20∼60 ppm of manganese concentration after 50 cycles between 3.6 V and 4.3 V with differential pulse polarography.[6] They also measured the amount of manganese with different applied potentials during storage conditions (up to 1800 minutes), which measured up to 41 ppm at 4.2 V. However, Xia et al. measured 1540 ppm of manganese concentration after 50 cycles between 3.5 V and 4.5 V at the room temperature and 7000 ppm of manganese at 50°C.[26] We carefully selected a range of manganese concentrations from 50 to 200 ppm in our study which is a reasonable representative range of manganese concentrations according to most literatures. In order to investigate the direct impact of manganese ions on the graphite electrode, the desired concentrations of manganese were dissolved in the electrolyte in advance. 50, 100, 150 and 200 ppm of $Mn(PF_6)_2$ were added into an electrolyte composed of 1M of $LiPF_6$ salt (Sigma-Aldrich) in ethylene carbonate (EC, Sigma-Aldrich) and dimethyl carbonate (DMC, Sigma-Aldrich) of 1:1 solvent mixtures to achieve the target concentration of manganese in the electrolyte. The $Mn(PF_6)_2$ salt was synthesized by reacting silver hexafluorophosphate ($AgPF_6$, Sigma-Aldrich) with the manganese chloride ($MnCl_2$, Sigma-Aldrich) in ethanol. The mixture was distilled to isolate the synthesized $Mn(PF_6)_2$. The moisture in $Mn(PF_6)_2$ was removed by heating it in a vacuum oven overnight at 90°C. The exact concentration of manganese in the electrolyte was measured with ICP-OES. In order to confirm that there is no additional source of supply of manganese ions, the total amount of manganese was measured for three samples after disassembly. The total amount of manganese after disassembly of the cell was very similar to the amount that was added to the electrolyte.

Electrochemical measurements.—

1. Cyclic voltammetry was applied to the lithium foil/graphite composite electrode half-cell to measure redox currents and current peak changes immediately following the addition of different concentrations of manganese. CV was carried out at 0.5 mV/s between 0.1 V and 3.0 V. Interfacial currents and current peaks were measured.
2. Capacity was measured using graphite/lithium half-cells at C/10 from 0.1 V to 0.9 V for 20 cycles. Additionally, some new cells were cycled at C/100 from 2.0 V to 3.0 V, which is above the deposition potential of Mn/Mn(II) (1.87 V vs. Li/Li^+), in order to prevent manganese deposition.
3. EIS measurements were performed to measure impedance change due to different concentrations of manganese and different potential of the graphite/electrolyte interface after the capacity was measured. Each concentration of manganese was measured with EIS at different voltages (0.1, 0.3, 0.5, 0.7 and 0.9 V) and different manganese concentrations (0, 50, 100, 150 and 200 ppm) in the electrolyte. Before conducting EIS measurements, the cells were rested in the open circuit voltage (OCV) condition for 2 hours to achieve stabilized potentials. AC impedance spectra were obtained by applying sinusoidal waves with amplitude of 5 mV over frequencies ranging from 100 kHz to 10 mHz.

ICP-OES measurements.—In order to determine the correlation between manganese deposition and capacity retention, the amount of manganese deposited on the graphite was measured after the capacity of the cells was measured. After disassembly from the coin cells, the cycled graphite electrodes were immersed in 25% nitric acid in water for 24 hours to extract the manganese. Next, ICP-OES measurements were carried out on the dissolved manganese from the graphite using a Perkin-Elmer Optima 2000 DV. Also, the amount of lithium that was deintercalated from the lithiated graphite was measured as a function of manganese concentration in the electrolyte. The graphite negative electrode was discharged with lithium metal (a reference electrode) and held at 0.05 V (x is about 0.9 in Li_xC_6) for 3 hours before storage to achieve lithiated graphite electrodes. Samples were stored in 1 mL of EC: DMC (1:1 by volume) with 0, 50 and 100 ppm of manganese ions at room temperature for 7 and 14 days.

SEM and EDS measurements.—The coin cells were first made with Li metal as a negative electrode and manganese metal as a positive electrode with 1M of $LiPF_6$ in EC: DMC (1:1 by volume) electrolyte and then cycled using the potentiodynamic cycling method. The cycled manganese metal surface was cleaned with DMC and scanned using SEM. SEM characterizations were carried out using a FEI Nova 200 NanoLab operating at 20 kV with a Schottky field emitter. Next, an elemental analysis was performed on the manganese metal surface by EDS. EDS analyses were performed using a FEI Nova 200 NanoLab attached with an energy dispersive X-ray spectrometer.

Results and Discussion

Cyclic voltammetry measurements of fresh graphite electrodes with different concentrations of manganese ions.—Figure 1 shows the results of cyclic voltammetry for the fresh graphite electrode with 0, 100 and 200 ppm of manganese ions in the graphite/lithium half-cell during the 1st cycle, the 10th cycle, and the 20th cycle. In the two-electrode cell lithium metal was used as both the counter and the reference electrode. While a three-electrode cell would give more precise potential relative to a reference electrode, it is difficult to achieve in a coin cell setup so two electrode cells have been widely used. We expect the difference between two and three electrode cells to be small since we used an excessive amount of lithium foil and the current in our experiment was small. In addition, our aim was to identify well-known current peaks instead of focusing on the precise potential of the electrode relative to a reference, so two-electrode cells were sufficient for this purpose.

First, in Figure 1 we can clearly observe changes in the peaks of anodic and cathodic currents depending on the concentration of manganese ions. Region A can be interpreted as the electrolyte reduction, SEI formation and manganese deposition peak, whereas B and C represent lithium intercalaction and deintercalation peak regions, respectively. Higher concentrations of manganese ions in the electrolyte caused increases in the cathodic current at potentials between 2.0 V and 0.5 V and decreases in the anodic current peak located between 0.3 V and 0.6 V as well as in the cathodic current peak located near 0.1 V to 0.3 V. Manganese deposition occurred during the reductive current scan below the standard redox potential of Mn/Mn(II), which is about 1.87 V (vs. Li/Li^+). After the manganese was deposited, subsequent electrolyte reduction reactions followed in the potential region of 0.8 V to 0.6 V. In the potential range of 0.5 V to 0.2 V, co-intercalation of the solvent and subsequent reduction of the electrolyte molecules occurred while forming the SEI layer.[28] During SEI formation, electrolyte decomposition products such as $(CH_2OCO_2Li)_2$, ROLi, and LiF were generated on the graphite surface.[29] However, due to the higher reactivity of manganese metal on the surface, the electrolyte reduction accelerated more violently with higher concentrations of manganese ions in the electrolyte. Due to the additional electrolyte reduction and manganese deposition reactions, decomposed layers might grow thicker and hinder lithium ions from the intercalation/deintercalation process. Consequently, the ability for lithium to (de)intercalate into the graphite would decrease considerably. It can be seen in Figure 1a that the cathodic current at potentials between 0.2 V and 0.1 V and the anodic current at potentials between 0.1 V and 0.4 V (where lithium intercalation/deintercalation reactions dominated) decreased significantly with higher concentrations of manganese ions.

Next, manganese ions in the electrolyte created additional reaction during the initial cycling. Figure 1a shows that with manganese ions in the electrolyte, the anodic current peak between 0.3 V and 0.6 V decreased while broadening, and shifted slightly to the higher potential region.

Finally, as the cycle number increased, the redox current related to side reactions such as electrolyte reduction and manganese deposition decreased, while the current related to lithium deintercalation increased. We extracted relevant peaks of the CV curves in Figure 1 and plotted them in Figure 2 as a function of the cycle number.

Downloaded on 2017-12-01 to IP 35.3.99.1 address. Redistribution subject to ECS terms of use (see ecsdl.org/site/terms_use) unless CC License in place (see abstract).

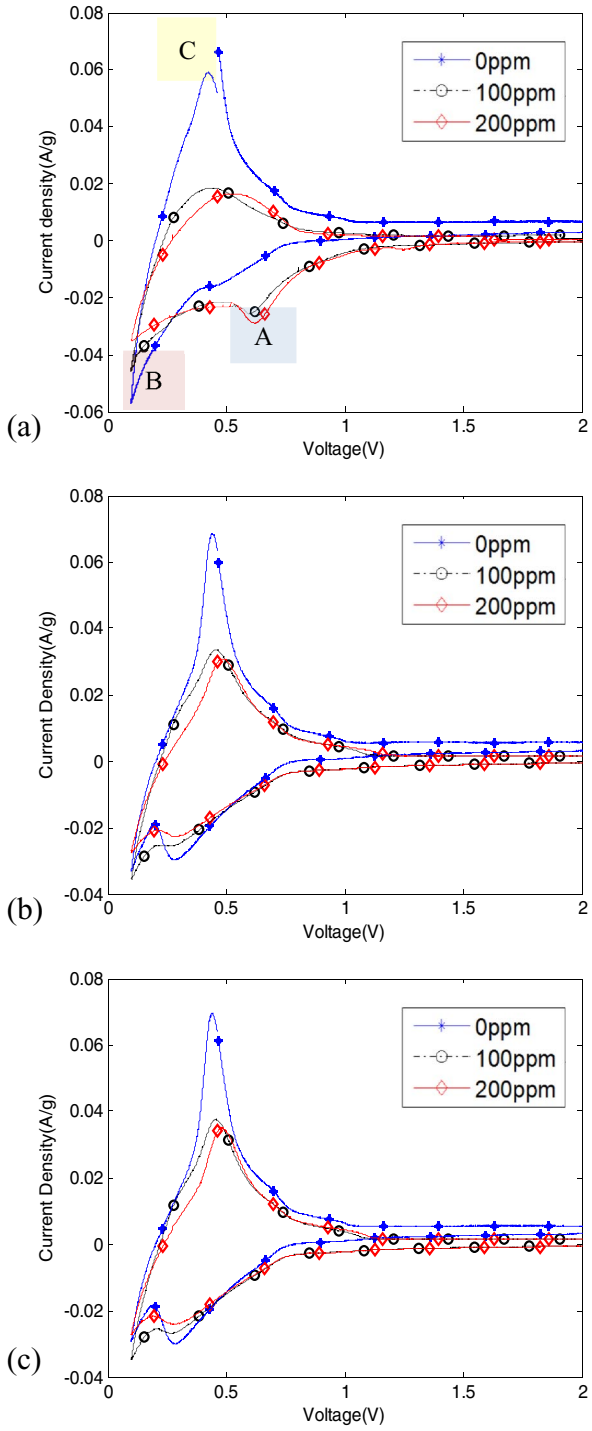

Figure 1. Cyclic voltammetry of fresh graphite electrode by adding different concentrations of manganese ions into the electrolyte in the graphite/lithium cell. (a) 1st cycle, (b) 10th cycle, (c) 20th cycle. Cyclic voltammetry was carried out at 0.5 mV/s between 0.1 V and 3.0 V.

Figure 2a shows that the reductive current peak at potentials between 2.0 V and 0.5 V, which corresponds to manganese deposition and electrolyte reduction, decreased significantly after the first cycle. Figure 2b shows that the anodic current peak related to lithium deintercalation, which was located between 0.3 V and 0.6 V, increased with the cycle number. This increase of the anodic current peak can be attributed to the slow wetting process of the active material[30] and the subsequent progressive change toward a stable SEI layer on graphite.[31] By comparing the figures in Figure 1, we can also observe that the anodic current peak became narrower with the cycle number.

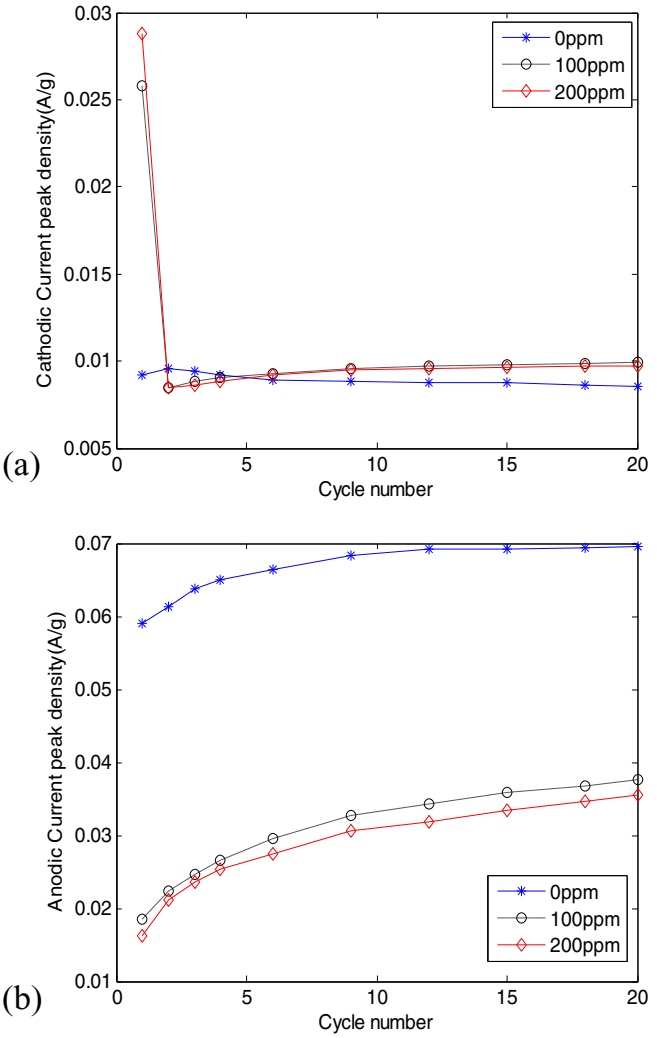

Figure 2. Change of current peaks with cycle number from fresh graphite/lithium cell added with different concentrations of manganese ions. Shown are (a) cathodic current peak at region A in Figure 1, and (b) anodic current peak at region C in Figure 1. Cyclic voltammetry was carried out at 0.5 mV/s between 0.1 V and 3.0 V.

Cyclic voltammetry measurements of formation-cycled graphite electrodes with different concentrations of manganese ions.—Figure 3a shows the CV curve in the 1st cycle right after adding different concentrations of manganese ions into lithiated graphite/lithium cell. Since the formation-cycled graphite samples contained lithium ions in the particles before the cell was reassembled, redox currents associated with the lithium deintercalation process were significantly larger than those in Figure 1. In the 1st cycle we can see that a higher concentration of manganese ions resulted in an increase of the anodic current in the peak region. Interestingly, this trend is opposite to that of fresh graphite electrodes, where a higher concentration of manganese ions resulted in a decrease of the anodic current in the peak region. This difference highlighted the significance of the state of the electrodes, where the formation-cycled graphite electrodes in Figure 3a were lithiated to start with.

Figure 3b shows the cyclic voltammetry curves at the 5th cycle after adding different concentrations of manganese ions to formation-cycled lithiated graphite. Similar to the fresh graphite electrode, we found that a higher concentration of manganese caused a decrease

Downloaded on 2017-12-01 to IP 35.3.99.1 address. Redistribution subject to ECS terms of use (see ecsdl.org/site/terms_use) unless CC License in place (see abstract).

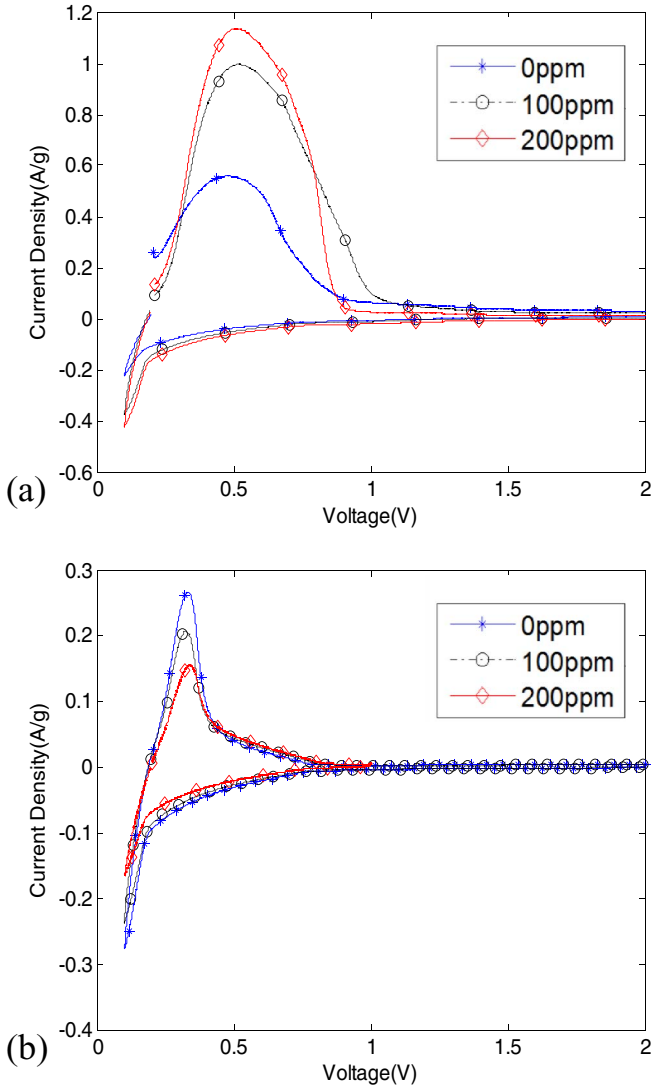

Figure 3. Cyclic voltammetry of formation-cycled graphite by adding different concentrations of manganese ions into the electrolyte in the lithiated graphite/lithium cell. (a) 1st cycle, (b) 5th cycle. The process involves formation cycling and voltage holding to get lithiated graphite, cell disassembly to use electrolyte added with different concentrations of manganese ions, and cell reassembly. Cyclic voltammetry was carried out at 0.5 mV/s between 0.1 V and 3.0 V.

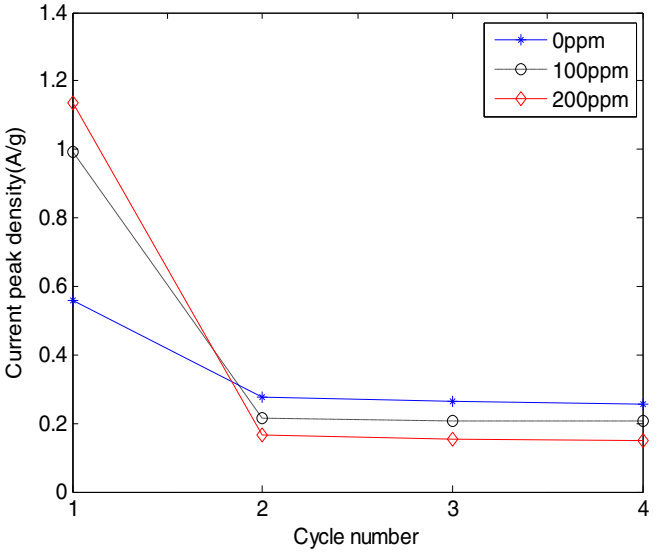

Figure 4. Change of anodic current peak with cycle number from formation-cycled lithiated graphite/lithium cell added with different concentrations of manganese ions.

in reversible lithium intercalation/deintercalation currents. Both the cathodic and anodic current peaks with a higher concentration of manganese ions were smaller than those with a lower concentration of manganese ions. Smaller interfacial currents can be interpreted as a decrease of the amount of lithium insertion/deinsertion into the graphite, resulting in capacity fade. As a result, higher concentrations of manganese ions in the cell cause a reduction of reversible interfacial currents.

We found that higher concentrations of manganese in the electrolyte led to higher anodic current peaks in the 1st cycle, but lower peaks in and after the 2nd cycle, as shown in Figure 4. This suggests that manganese ions contributed to an increase of the anodic current peak before manganese deposition occurred. The current peak decreased remarkably after the 1st cycle and stabilized in subsequent cycles. The higher anodic current associated with the higher concentration of manganese in the 1st cycle suggests that more irreversible oxidative reaction occurred during the first CV cycle right after adding manganese ions into the cell. We found that manganese ions have a positive effect on cell performance by increasing the redox current before the manganese ions deposit onto the graphite. However, the cathodic and anodic currents significantly decreased right after the reductive scan was finished.

Figure 5a shows the CV curves in the 1st cycle after adding manganese ions into the formation-cycled delithiated graphite/lithium cell. The anodic and cathodic currents decreased remarkably after reassembly of the cell, especially at higher concentrations of manganese ions. These results are in contrast to those in Figure 3a, which used lithiated graphite for the anode. A higher concentration of manganese caused a dramatic increase in the interfacial current in the lithiated graphite, whereas it caused a decrease in the delithiated graphite electrode. Our hypothesis of this difference is that manganese facilitated lithium deinterlacation in the lithiated graphite which had lots of initially intercalated lithium ions to work with during the first cycle. After the first cycle, the effect was dominated by manganese deposition which reduced the interfacial current.

The CV curves in the 5th cycle with different concentrations of manganese ions in formation-cycled delithiated graphite are shown in Figure 5b. Comparing to Figure 5a, the peak of anodic current increased while the peak of cathodic current for lithium intercalation decreased. Higher concentrations of manganese ions in the electrolyte caused a larger decrease in interfacial currents. It is expected that manganese ions deposited relatively fast onto the graphite surface because of the higher standard redox potential of Mn/Mn(II) (1.87 V vs. Li/Li^+) compared to the potential of lithium intercalation into graphite (< 0.3 V vs Li/Li^+). Deposited manganese may react with other components such as C and O originating from electrolyte reduction and form another electrolyte interface layer containing manganese. Manganese deposition on graphite not only forces cyclable lithium to deintercalate from the graphite, but also induces electrolyte reduction reactions, both of which result in significant capacity fade. The reduction of exchange current associated with lithium intercalation/deintercalation at higher concentrations of manganese ions also negatively impacts the power performance.

By comparing the CV results of fresh, lithiated and de-lithiated graphite electrodes, we can obtain several important observations. The major difference among these results can be found in the A and the C regions of the CV curves. An increase of the cathodic current peak in region A with the manganese concentration was only observed in fresh graphite electrodes. This region is mainly caused by electrolyte reduction and SEI formation, which are significantly influenced by manganese ions. It is very likely that manganese ions

Downloaded on 2017-12-01 to IP 35.3.99.1 address. Redistribution subject to ECS terms of use (see ecsdl.org/site/terms_use) unless CC License in place (see abstract).

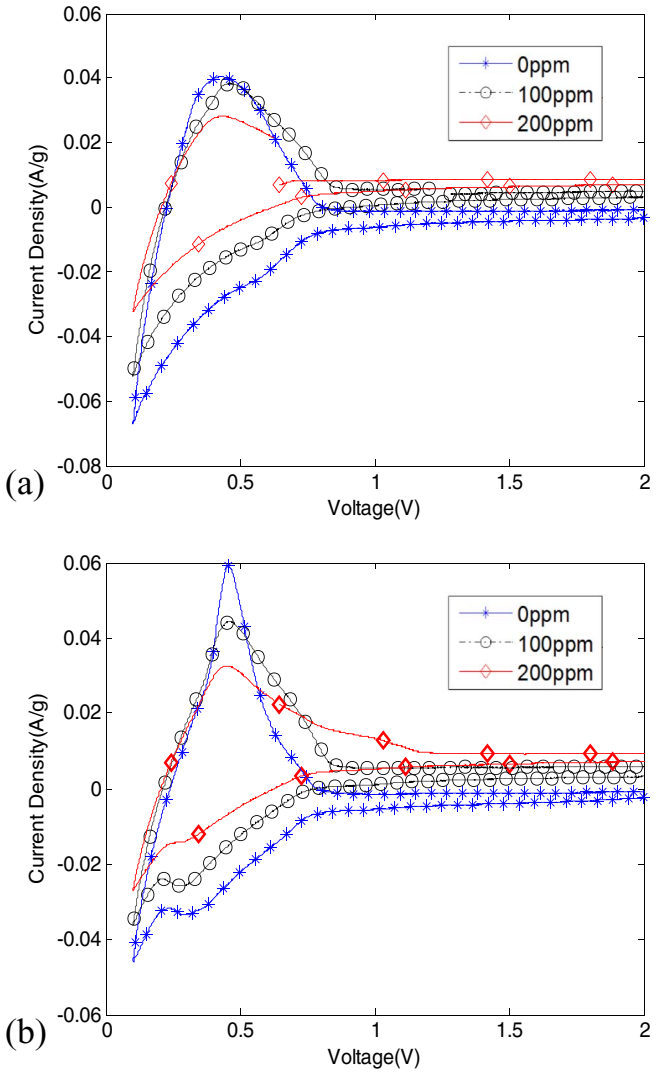

Figure 5. Cyclic voltammetry of formation-cycled graphite by adding different concentrations of manganese ions into the electrolyte in the delithiated graphite/lithium cell. (a) 1st cycle, (b) 5th cycle. The process involves formation cycling and voltage holding to get delithiated graphite, cell disassembly to use electrolyte added with different concentrations of manganese ions, and cell reassembly. Cyclic voltammetry was carried out at 0.5 mV/s between 0.1 V and 3.0 V.

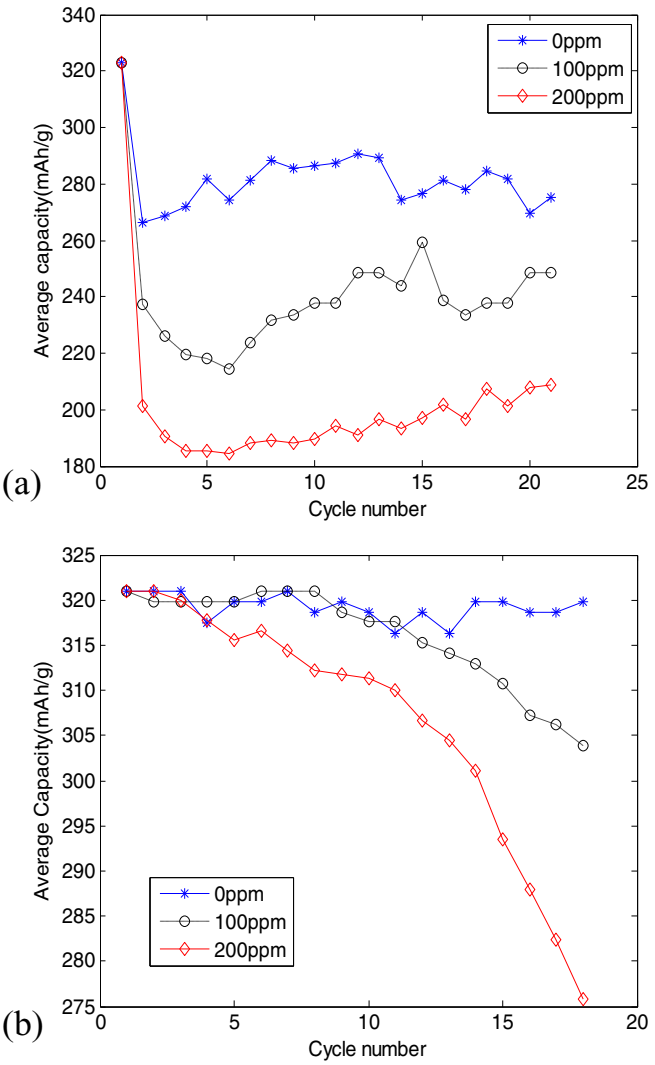

Figure 6. Change of (a) charge and (b) discharge capacity of fresh graphite electrode with cycle number after adding 0, 100 and 200 ppm of manganese ions in the electrolyte.

accelerate electrolyte reduction and SEI formation when SEI layers are forming. However, these cathodic peaks disappear after SEI layers are formed, which suggests an ending of aggressive electrolyte reduction following SEI formation. An increase of the anodic peak in region C with the manganese concentration was only observed in lithiated graphite electrodes during the first cycle. Delithiated graphite electrodes showed an opposite trend. A common observation is that the anodic current peak in region C decreased with the manganese concentration after the first cycle.

Capacity measurements of fresh graphite electrodes with different concentrations of manganese ions.—Figure 6 shows the charge and discharge capacity of fresh graphite electrodes after adding different concentrations of manganese into the cell.

In the 1st cycle, the charge capacity decreased significantly due to SEI growth and irreversible electrochemical decomposition of the electrolyte. This phenomenon is known as irreversible charge loss (ICL) originating from solvent reduction and SEI formation, which is one of the major characteristics of the SEI layer.[29] However, higher concentrations of manganese ions in the electrolyte caused significant irreversible loss of charge capacity when forming SEI layer on the graphite electrode. For example, the charge capacity of the cell decreased by 37% with 200 ppm of manganese ions and by only 17% when no manganese ions was added, as shown in Figure 6a. It is highly likely that manganese ions in the electrolyte were deposited earlier due to the higher standard potential as compared to electrolyte reduction and SEI layer formation. Higher reactivity of deposited manganese can induce additional electrolyte reduction and growth of decomposed layers. The charge capacity became stable after the initial SEI layers were formed.

The discharge capacity during the first few cycles does not decrease as significantly as the charge capacity.[32] Still, the discharge capacity of the graphite electrode decreased continuously during the 20 cycles, as shown in Figure 6b. It is obvious that higher concentrations of manganese ions caused greater capacity decrease. In the early stage, adding 200 ppm manganese ions in comparison to adding 100 ppm manganese ions does not appear to cause an immediate conspicuous difference on the capacity or the CV curve. However, this can affect longer term continuous degradation by harming the passivation effect of the SEI layer. As can be seen in Figure 6b, the capacity difference between adding 100 ppm and 200 ppm is not significant in the early stage, but increases to about 10% after 20 cycles. After 20 cycles, there was about 15% of capacity decrease with 200 ppm of manganese ions

Downloaded on 2017-12-01 to IP 35.3.99.1 address. Redistribution subject to ECS terms of use (see ecsdl.org/site/terms_use) unless CC License in place (see abstract).

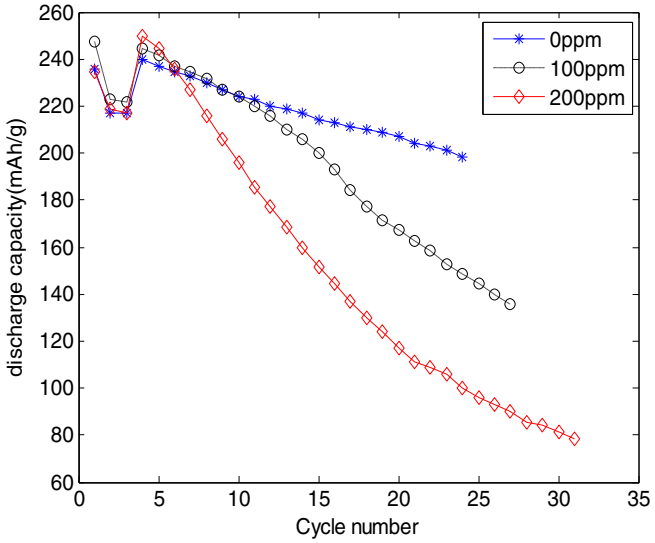

Figure 7. Change of discharge capacity of lithiated graphite electrode before and after adding 0, 100 and 200 ppm of manganese ions in the electrolyte. Cycled lithiated graphite electrode was disassembled and reassembled with electrolyte of added manganese ions after the 3rd cycle. Different manganese concentrations take effect since the 4th cycle.

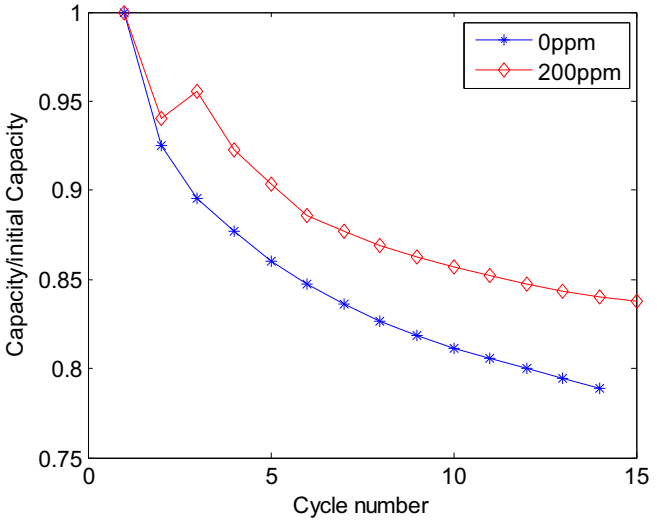

Figure 8. Discharge capacity of cycled lithiated graphite reassembled with and without manganese ions. The cells were cycled between 2.0 V to 3.0 V with C/100 rate to avoid manganese deposition and electrolyte reduction. The cycled lithiated graphite electrode was reassembled after the 2nd cycle. It was found that manganese ions contribute to increasing discharge capacity if they do not deposit on the graphite and provoke side reactions.

in the electrolyte. Presumably, deposited manganese with electrolyte decomposition products on the graphite surface hindered the lithiation/delithiation process during cycling, which affected the unceasing decline of the discharge capacity of the cell. Moreover, the capacity of the cells kept decreasing as the cycle number increased, which means that passivation of the SEI layer was not fully established on the graphite surface. These results agreed with the previous study,[20] which proposed that high electronic conductivity of the manganese metal formed on the graphite surface might be the reason for this lack of passivation effect.

Capacity measurement formation-cycled graphite electrodes with different concentrations of manganese ions.—Capacity change of formation-cycled graphite electrode was measured before and after adding different concentrations of manganese ions in the electrolyte, as shown in Figure 7. Because the cyclable lithium ions resided in the lithiated graphite electrode, the capacity slightly increased during the 4th cycle when the cell was reassembled after the formation cycle. Consistent with the previous CV findings using lithiated graphite (which determined that the redox current increased due to oxidative reaction), capacity increased more when higher concentrations of manganese in the electrolyte were added to the cell. Increases of discharge capacity were probably due to the additional electrons coming from oxidative reaction right after the addition of manganese ions. However, in subsequent cycles the rate of capacity decrease with higher concentrations of manganese ions was significantly higher than that of the lower manganese concentration. It seems that the manganese ions in the electrolyte increase capacities in the cell initially, which positively affect the cell during initial cycling before manganese deposition. However, manganese deposition and consequent side reactions eventually increase the rate of capacity decrease. For instance, more than 50% of the capacity decreased after 20 cycles, when 200 ppm of manganese ions were added into the cell.

In order to support the claim that manganese ions improve capacity and cell performance before they deposit onto the graphite, additional experiments were performed. Cycled lithiated graphite was reassembled with and without manganese ions and cycled between 2.0 V to 3.0 V with C/100 rate to avoid manganese from depositing and inducing side reactions on the graphite surface. Upon discharge of the lithiated graphite electrode, oxidative reaction should occur when the voltage rises from 0.1 V to 3.0 V. However, manganese deposition and electrolyte reduction is avoided by limiting the potential window from 3.0 V to 2.0 V of the cathodic current. C/100 charge and discharge rate was used in this experiment since the amount of lithium which can be inserted into the graphite is very limited. Figure 8 shows the discharge capacity of graphite before and after adding 0 ppm and 200 ppm of manganese ions into the electrolyte, respectively. It is obvious that manganese ions contribute to increase discharge capacity if they do not deposit on the graphite and provoke side reactions.

Electrochemical Impedance Spectroscopy (EIS) measurements.—Typical impedance spectra for a graphite composite electrode composed of a semicircle with an inclined slope as can be seen in Figure 9. The EIS measurement was performed after the 20 cycles of capacity measurement. By separating the frequency region of the EIS spectra, reactions and electrochemical characteristics of the electrode and electrolyte can be identified.[33–36] We adopted a simple model from the previous literature[33] to quantify the ohmic resistance, charge transfer resistance and lithium diffusion. The left end point of the semicircle in the higher frequency domain relates to the ohmic resistance of the electrode and electrolyte, while the radius of the semicircle in the mid-range frequency zone is the charge-transfer reaction at the electrolyte/electrode interface. The inclined line connected to the semicircle on the right indicates the diffusion of lithium. Figures 9a and 9b show the EIS spectra with different concentrations of manganese ions in the electrolyte at 0.1 V and 0.7 V, respectively. Impedance spectra shift to the right as the concentration of manganese ions in the electrolyte increases, implying an increase of ohmic resistance. Moreover, the radius of the impedance spectra semi-circle also increased, which is closely related to the charge transfer resistance of the cell. It can be seen in Figure 9b that the slope in the diffusion region of the impedance spectra connecting to the semi-circle on the right decreases with the manganese concentration. This indicates that lithium diffusion is retarded by manganese ions.

In order to quantify the changes of impedances induced by manganese ions more thoroughly, we extracted the ohmic and charge transfer resistances in Figure 9 and plotted them in Figure 10 as a function of the concentration of manganese ions in the electrolyte. We can observe in Figure 10a that the ohmic resistance is increased by about 134% while the charge transfer resistance is increased by about 44% at 0.1 V after adding 200 ppm of manganese ions to the

Downloaded on 2017-12-01 to IP 35.3.99.1 address. Redistribution subject to ECS terms of use (see ecsdl.org/site/terms_use) unless CC License in place (see abstract).

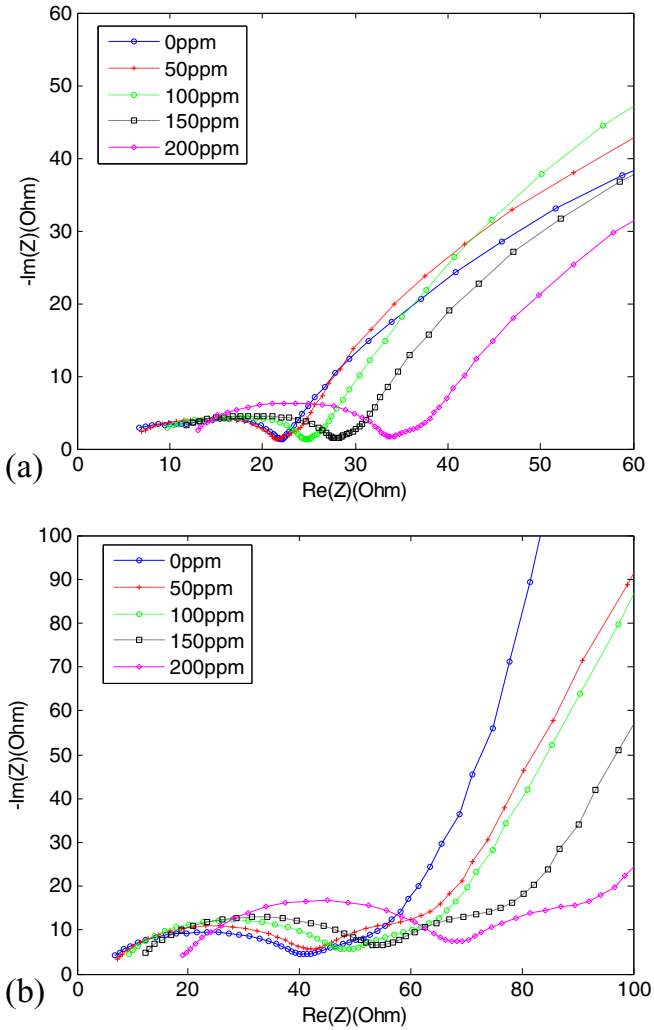

Figure 9. EIS spectra with 0, 50, 100, 150 and 200 ppm of manganese ions in the electrolyte at (a) 0.1 V and (b) 0.7 V. AC impedance spectra were obtained by applying the waves with amplitude of 5 mV over a frequency range from 100 kHz to 10 mHz.

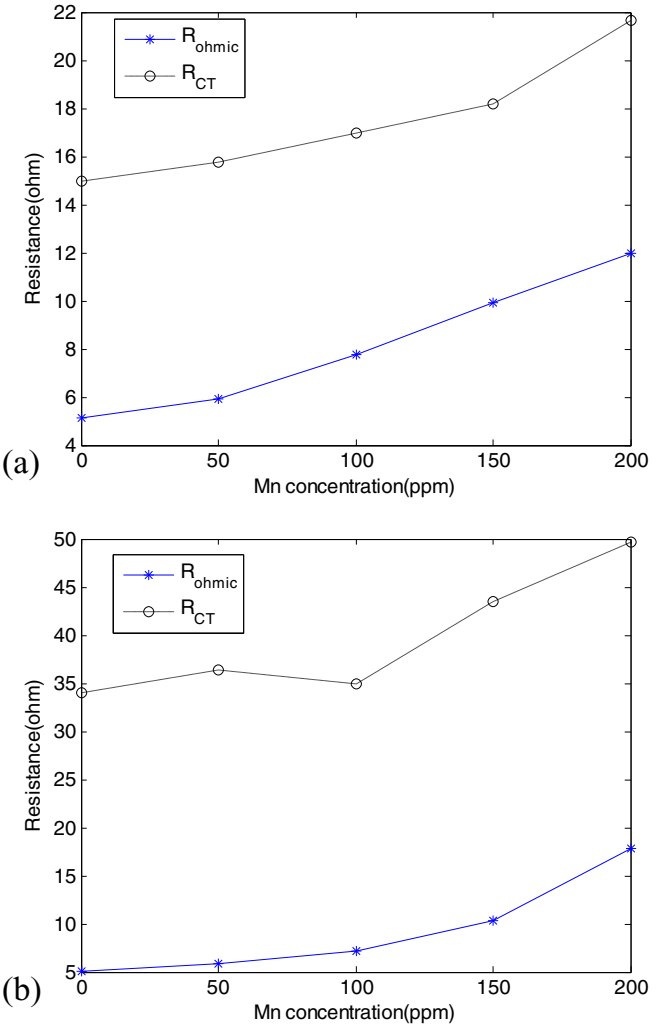

Figure 10. Ohmic and charge transfer (CT) resistance of the graphite electrode at (a) 0.1 V and (b) 0.7 V after adding different concentrations of manganese ions in the electrolyte. AC impedance spectra were obtained by applying the waves with amplitude of 5 mV over a frequency range from 100 kHz to 10 mHz. Ohmic resistance was measured at 100 kHz and charge transfer resistance was measured at 15 Hz.

electrolyte. Similar trend of increasing resistance with the manganese concentration can also be observed in Figure 10b. It is well known that LiF generated from the salt reduction and $ROCO_2Li$ formed by the solvent reaction are the main contributors for increasing interfacial resistance at the surface of graphite.[2] These electrolyte and salt reduction processes will be accelerated when manganese ions are present in the electrolyte by depositing as a metallic state and acting as a catalyst on the graphite surface. The deposited manganese contributes to increasing the ohmic resistance by forming an additional interfacial layer and to increasing the charge transfer resistance by impeding the lithium intercalation/deintercalation process. Higher manganese concentration leads to a thicker interfacial layer, which causes more increase of the ohmic and charge transfer resistances. These reactions will continuously degrade cell performance and reduce cell capacity.

Figures 11a and 11b show the EIS spectra at different voltages with 0 ppm and 50 ppm of manganese in the electrolyte, respectively. High frequency resistance remained similar throughout the voltage range. Most of the impedance change was due to an increase of charge transfer resistance shown as the increase of the radius in the semicircle in the figure. As expected, the amount of lithium in the graphite continuously decreases as the voltage of the cell increases from 0.1 V to 0.9 V. Since different amounts of lithium are present in the graphite at different voltages, the charge-transfer resistance also changes with different voltages as expected because charge transfer resistance is SOC-dependent.

ICP-OES measurements for the amount of deposited manganese during cycling.—In order to validate the hypothesis that capacity and redox current peak decreased due to manganese deposition, the amount of manganese on the graphite was measured using ICP-OES after the capacities were verified. As expected, higher concentrations of manganese added into the cell result in larger amounts of manganese deposition on the graphite as shown in Table I. In addition, higher concentrations of manganese ions in the electrolyte contribute to larger discharge capacity loss as shown in Figure 6. Therefore, capacity decrease in the graphite anode increases with the amount of manganese ions added into the cell due to manganese deposition and its side reactions.

ICP-OES measurements for the amount of lithium loss during storage.—The concentration of lithium was measured to investigate the correlation between manganese ions in the electrolyte and the amount of lithium deintercalation from the lithiated graphite electrode. The lithiated graphite electrode was put into the electrolyte with different concentrations of manganese and stored for 7 and 14

Downloaded on 2017-12-01 to IP 35.3.99.1 address. Redistribution subject to ECS terms of use (see ecsdl.org/site/terms_use) unless CC License in place (see abstract).

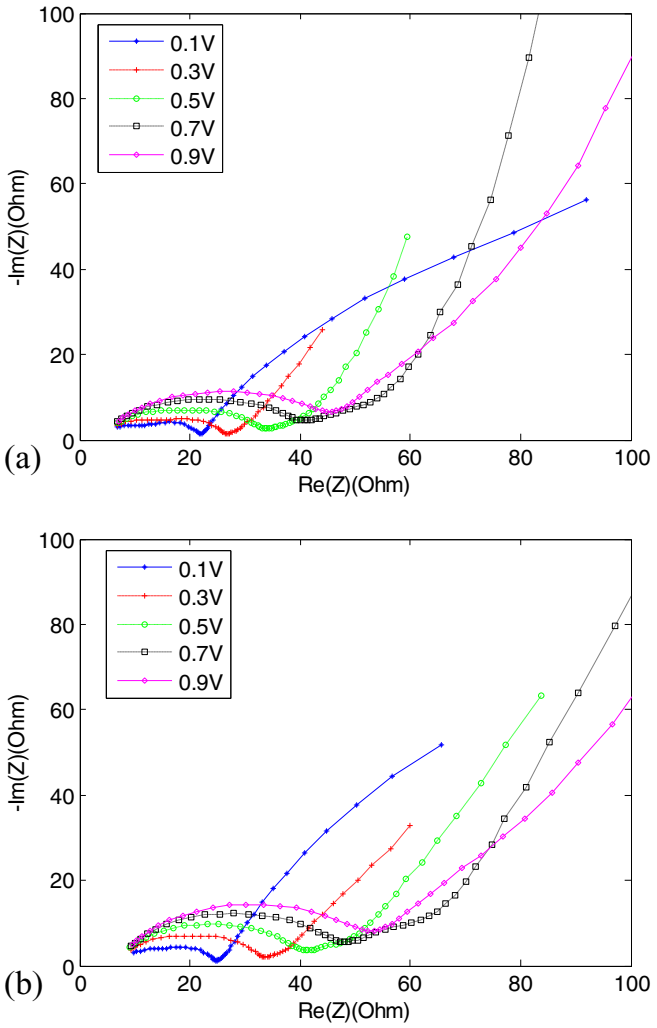

Figure 11. EIS spectra at 0.1, 0.3, 0.5, 0.7, and 0.9 V (vs. Li/Li^+) with adding (a) 0 ppm and (b) 50 ppm of manganese ions in the electrolyte. AC impedance spectra were obtained by applying the waves with amplitude of 5 mV over a frequency range from 100 kHz to 10 mHz.

days in order to observe the effect of manganese on the charged graphite anode. Table II shows the amount of deposited manganese on the graphite and the amount of lithium in the electrolyte measured using ICP-OES.

As expected, higher concentrations of manganese ions put into the electrolyte cause the deposition of more manganese on the graphite surface. Moreover, the amount of dissolved lithium in the electrolyte is increased if we put higher concentrations of manganese in the electrolyte. Even with 0 ppm of manganese in the electrolyte, 2.7 mols

Table I. Amount of manganese deposited on the graphite with different concentrations of manganese.

Manganese concentration (ppm)	Amount of manganese deposited on the graphite (ug)
50	8.7783
100	14.528
150	28.078
200	31.378

Measured by ICP-OES after the capacity measurement shown in Figure 6.

Table II. Amount of manganese deposited on the graphite and amount of dissolved lithium in the electrolyte.

Duration (days)	Mn concentration (ppm)	Amount of manganese deposited on graphite (umol)	Amount of dissolved lithium in electrolyte (umol)
7	0	0.00102	2.7492
7	50	0.10584	3.4841
7	100	0.17673	4.4027
14	0	0.00134	2.7564
14	50	0.11412	5.4639

The graphite negative electrode was discharged with lithium metal (a reference electrode) and held at 0.05V (x is about 0.9 in Li_xC_6) for 3 hours before storage to achieve lithiated graphite electrodes. Samples were stored in 1 mL of EC: DMC (1:1 by volume) with 0, 50 and 100 ppm manganese at room temperature for 7 and 14 days.

of lithium were dissolved into the electrolyte, which might be produced from lithium deintercalation due to the self-discharge of lithiated graphite. For instance, during long-term storage in open circuit voltage conditions, a current leakage will contribute to building the SEI layer by reacting with the electrolyte. Moreover, protic species coming from water are also reducible by consuming electrons from the graphite[8],

$$H^+ + e^- \rightarrow \frac{1}{2}H_2 \quad [1]$$

$$H_2O + e^- \rightarrow \frac{1}{2}H_2 + OH^- \quad [2]$$

In Table II we can clearly see the effect of manganese ions since the amount of lithium coming out from the graphite increased remarkably as a larger amount of manganese was deposited. Moreover, the number of mols of lithium deintercalated from the graphite was much more than the stoichiometric amount of lithium from the manganese-lithium exchange mechanism[9,12], or

$$yMn^{2+} + Li_xC_6 \rightarrow yMn + Li_{x-2y}C_6 + 2yLi^+ \quad [3]$$

These results show that manganese ions cause more than just manganese-lithium exchange, which appears to be only a small portion of the overall capacity degradation. It is supposed that the additional formation of decomposed layers induced by manganese deposition provokes lithium deintercalation and the generation of decomposed products which additionally consume lithium from the graphite electrode.

SEM and EDS measurements.—We predicted that deposited manganese metal induces the formation of decomposed layers with electrolyte reduction products on the graphite surface. In order to examine the hypothesis, microscopic observations and elemental analysis were conducted via SEM and EDS, respectively. For clear observation of the layer generated on the manganese metal surface, we replaced the graphite anode with manganese metal. Figure 12 and Figure 13 show the images of the manganese metal before and after cycling as well as the EDS spectra on the manganese surface. By comparing fresh and cycled manganese metal surfaces, it is clear that additional decomposed layers are formed on the manganese metal surface. From the EDS spectra analysis, C, F and P element were detected in the cycled manganese metal surface as seen in Figure 13b. These elements originate from the electrolyte decomposition product of the electrolyte and are the components of additional layers provoked by manganese metal surfaces. Similar processes can take place with the deposited manganese on the graphite anode surface.

In conclusion, it is obvious that manganese ions in the electrolyte provoke not only the dissolution of lithium in the electrolyte by reduction of manganese but also the formation of additional decomposed

Downloaded on 2017-12-01 to IP 35.3.99.1 address. Redistribution subject to ECS terms of use (see ecsdl.org/site/terms_use) unless CC License in place (see abstract).

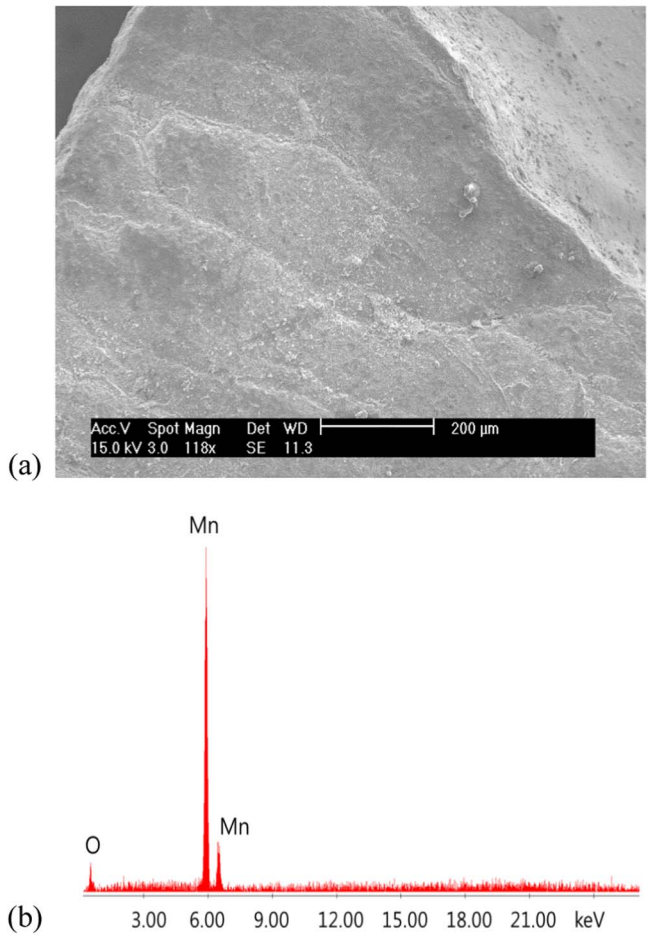

Figure 12. (a) Fresh Mn metal surface (b) EDS spectra on the fresh Mn surface.

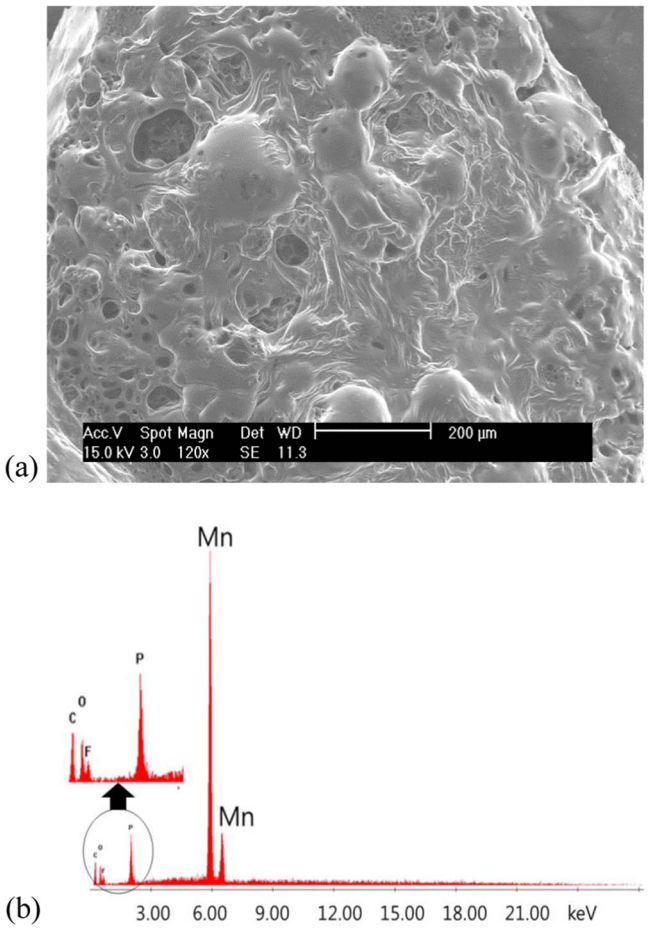

Figure 13. (a) Cycled Mn metal surface (b) EDS spectra on the cycled Mn surface.

layers with electrolyte reduction products on the graphite electrode surfaces. Due to the higher reactivity of manganese metal on the surface, electrolyte reduction accelerates more violently when higher concentration of manganese in the electrolyte is added to the cell. Moreover, the amount of lithium deintercalated from the graphite anode also increases due to manganese deposition. These processes will also contribute to form thicker decomposed layers on the graphite surface and hinder the lithium transport process, which causes an increase of ohmic and charge transfer resistances. All these side reactions cause significant irreversible interfacial currents and discharge capacity decrease, which should be prevented to improve the cycle life of the battery electrode. Previous studies have not reached consensus on the oxidation state of manganese present in the SEI layer of the graphite. Since Mn metal is very reactive, it might be difficult to detect the state from XPS. Also, manganese might be involved in the generation of Mn-containing SEI layer in the form of manganese compounds. This is probably why several XPS measurements only observed an oxide form of Mn,[4,13,14,20] whereas some studies observed metallic state of manganese.[12,21]

Based on the various measurements of different graphite samples, we summarize the effects of manganese ions on fresh, lithiated and delithiated graphite electrodes as follows:

1. Higher concentrations of manganese ions cause an increase in currents related to side reactions and a decrease in redox currents of reversible lithium intercalation/deintercalation reactions for fresh and cycled graphite electrodes after manganese deposition occurs. Moreover, the cell capacity decreases dramatically, while the cell impedance increases significantly.
2. Irreversible side reactions such as electrolyte reduction and manganese deposition dominate the reaction initially after adding manganese ions into the cell. However, reversible lithium intercalation/deintercalation reactions increase slightly while irreversible reactions fade away as the cycle number increases for fresh and cycled graphite electrodes. However, capacity decreases continuously as the cycle number increases, which is mainly caused by the rise of cell impedance and the lack of the passivation effect.
3. Capacity and redox current increase with manganese ions before they are deposited onto the graphite electrode and induce side reactions. However, right after manganese reduction, the redox current decreases dramatically. Our observations suggest that manganese deposition on graphite is one of the major causes of side reactions.

These interesting observations suggest that manganese ions in the electrolyte positively affect capacity and cell performance if they are not deposited onto the graphite surface. When cycling a battery using manganese-containing cathode material, the manganese ions will be continuously generated from the cathode material and deposited onto the graphite. Thus, different additives and coatings that prevent manganese deposition on the graphite might be one of the critical ways to improve capacity and cell performance.

Conclusions

In order to investigate the direct impact of manganese deposition and consecutive side reactions on the graphite anode, several complementary techniques were introduced. Each technique divulged a

Downloaded on 2017-12-01 to IP 35.3.99.1 address. Redistribution subject to ECS terms of use (see ecsdl.org/site/terms_use) unless CC License in place (see abstract).

specific aspect of the manganese deposition and its interaction with the electrolyte and the SEI layer. CV and capacity measurements have revealed that decomposition of the electrolyte gets accelerated when manganese ions are introduced, which also influences the SEI layer growth. The corresponding impedance rise has been confirmed by EIS measurements. We suggest that the formation of the decomposed layer is accelerated by formation of reactive metallic manganese on the graphite surface. Direct evidence supporting the hypothesis based on the electrochemical measurements has been found with ICP-OES, SEM, and EDS characterization. ICP-OES measurements have also confirmed that side reactions can be accelerated when the amount of deposited manganese in the graphite is increased. SEM and EDS measurements have been performed directly on the cycled metallic manganese surface, and it is observed that additional decomposed layers are formed with the electrolyte decomposition products. In addition, an interesting observation is that dissolved manganese ions are not harmful to battery cells before they are deposited into the anode. Capacity and redox current increase with manganese ions before they are deposited onto the graphite electrode and induce side reactions. However, right after manganese reduction, the redox current decreases dramatically. These results indicate that the reaction of manganese ions depends on the voltage conditions during charge or discharge and the lithiatiaon status of the graphite electrode. Further, non-passivation of the film layer contaminated by manganese, which can be estimated by the continuous decrease of discharge capacity, may be explained by the formation of metallic manganese. All these results highlight the importance of an integrated understanding of manganese deposition.

Acknowledgments

This work was supported by the National Science Foundation under grant No. CNS-1446117, and also partially supported by the Advanced Battery Coalition for Drivetrains at the University of Michigan. Support from our sponsor is gratefully acknowledged.

References

1. A. Manthiram, *The Journal of Physical Chemistry Letters*, **2**, 176 (2011).
2. P. Arora, R. E. White, and M. Doyle, *Journal of The Electrochemical Society*, **145**, 3647 (1998).
3. J. Shim, R. Kostecki, T. Richardson, X. Song, and K. A. Striebel, *Journal of Power Sources*, **112**, 222 (2002).
4. L. Yang, M. Takahashi, and B. Wang, *Electrochimica Acta*, **51**, 3228 (2006).
5. R. J. Gummow, A. de Kock, and M. M. Thackeray, *Solid State Ionics*, **69**, 59 (1994).
6. D. H. Jang and S. M. Oh, *Journal of The Electrochemical Society*, **144**, 3342 (1997).
7. E. Iwata, K. -i. Takahashi, K. Maeda, and T. Mouri, *Journal of Power Sources*, **81–82**, 430 (1999).
8. A. Biyr and C. Sigala, *Journal of The Electrochemical Society*, **145**, 194 (1998).
9. H. Tsunekawa, S. Tanimoto, R. Marubayashi, M. Fujita, K. Kifune, and M. Sano, *Journal of The Electrochemical Society*, **149**, A1326 (2002).
10. T. Tsujikawa, K. Yabuta, T. Matsushita, M. Arakawa, and K. Hayashi, *ECS Transactions*, **25**, 309 (2010).
11. S. Komaba, N. Kumagai, and Y. Kataoka, *Electrochimica Acta*, **47**, 1229 (2002).
12. M. Ochida, Y. Domi, T. Doi, S. Tsubouchi, H. Nakagawa, T. Yamanaka, T. Abe, and Z. Ogumi, *Journal of The Electrochemical Society*, **159**, A961 (2012).
13. H. Shin, J. Park, A. M. Sastry, and W. Lu, *Journal of Power Sources*, **284**, 416 (2015)
14. C. Zhan, J. Lu, A. J. Kropf, T. Wu, A. N. Jansen, Y. -K. Sun, X. Qiu, and K. Amine, *Nature Communications*, **4**, 2437 (2013).
15. J. Wandt, A. Freiberg, R. Thomas, Y. Gorlin, A. Siebel, R. Jung, H. A. Gasteiger, and M. Tromp, *Journal of Materials Chemistry A*, **4**, 18300 (2016).
16. D. P. Abraham, T. Spila, M. M. Furczon, and E. Sammann, *Electrochemical and Solid-State Letters*, **11**, A226 (2008).
17. D. R. Vissers, Z. Chen, Y. Shao, M. Engelhard, U. Das, P. Redfern, L. A. Curtiss, B. Pan, J. Liu, and K. Amine, *ACS Applied Materials & Interfaces*, **8**, 14244 (2016).
18. I. Belharouak, G. M. Koenig Jr., T. Tan, H. Yumoto, N. Ota, and K. Aminea, *Journal of The Electrochemical Society*, **159**(8) A1165 (2012).
19. Y. Shilina, B. Ziv, A. Meir, A. Banerjee, S. Ruthstein, S. Luski, D. Aurbach, and I. C. Halalay, *Analytical Chemistry*, **88**, 4440 (2016).
20. C. Delacourt, A. Kwong, X. Liu, R. Qiao, W. L. Yang, P. Lu, S. J. Harris, and V. Srinivasan, *Journal of The Electrochemical Society*, **160**, A1099 (2013).
21. M. Ochida, T. Doi, Y. Domi, S. Tsubouchi, H. Nakagawa, T. Yamanaka, T. Abe, and Z. Ogumi, *Journal of The Electrochemical Society*, **160**, A410 (2013).
22. X. Xiao, Z. Liu, L. Baggetto, G. M. Veith, K. L. More, and R. R. Unocic, *Physical Chemistry Chemical Physics*, **16**, 10398 (2014).
23. S. R. Gowda, K. G. Gallagher, J. R. Croy, M. Bettge, M. M. Thackeray, and M. Balasubramanian, *Physical Chemistry Chemical Physics*, **16**, 6898 (2014).
24. I. A. Shkrob, A. J. Kropf, T. W. Marin, Y. Li, O. G. Poluektov, J. Niklas, and D. P. Abraham, *The Journal of Physical Chemistry C*, **118** , 24335 (2014).
25. T. Inoue and M. Sano, *Journal of The Electrochemical Society*, **145**, 11 (1998).
26. Y. Xia, Y. Zhou, and M. Yoshio, *Journal of The Electrochemical Society*, **144**, 8 (1997).
27. L. Wang, C. C. Ou, K. A. Striebel, and J. -S. Chen, *Journal of The Electrochemical Society*, **150**, A905 (2003).
28. J. Li, H. Su, L. Huang, and S. Sun, *Science China Chemistry*, **56**, 992 (2013).
29. P. Verma, P. Maire, and P. Novák, *Electrochimica Acta*, **55**, 6332 (2010).
30. M. D. Levi, E. Levi, Y. Gofer, D. Aurbach, E. Vieil, and J. Serose, *The Journal of Physical Chemistry B*, **103**, 1499 (1999).
31. E. Markevich, V. Baranchugov, G. Salitra, D. Aurbach, and M. A. Schmidt, *Journal of The Electrochemical Society*, **155**, A132 (2008).
32. C. Wang, A. J. Appleby, and F. E. Little, *Journal of Electroanalytical Chemistry*, **497**, 33 (2001).
33. W. Waag, S. Käbitz, and D. U. Sauer, *Applied Energy*, **102**, 885 (2013).
34. M. Schönleber, C. Uhlmann, P. Braun, A. Weber, and E. Ivers-Tiffée, *Electrochimica Acta*, **243**,250 (2017).
35. D. Aurbach, B. Markovsky, I. Weissman, E. Levi, and Y. Ein-Eli, *Electrochimica Acta*, **45**, 67 (1999).
36. M. A. Monem, K. Trad, N. Omar, O Hegazy, B. Mantels, G. Mulder, P. V. Bossche, and J. V. Mierlo, *Applied Energy*, **152**, 143 (2015).

Downloaded on 2017-12-01 to IP **35.3.99.1** address. Redistribution subject to ECS terms of use (see **ecsdl.org/site/terms_use**) unless CC License in place (see abstract).